Journal of Cerebral Blood Flow & Metabolism (2014) 34, 242–247

www.jcbfm.com

ORIGINAL ARTICLE

Cerebrovascular reactivity in the brain white matter: magnitude, temporal characteristics, and age effects

Binu P Thomas[1,2,3], Peiying Liu[1,4], Denise C Park[5], Matthias JP van Osch[6] and Hanzhang Lu[1,2,3,4]

White matter (WM) comprises about half of the brain and its dysfunction is implicated in many brain disorders. While structural properties in healthy and diseased WM have been extensively studied, relatively little is known about the physiology underlying these structural characteristics. Recent advances in magnetic resonance (MR) technologies provided new opportunities to better understand perfusion and microvasculature in the WM. Here, we aim to evaluate vasodilatory capacity of the WM vasculature, which is thought to be important in tissue ischemia and autoregulation. Fifteen younger and fifteen older subjects performed a CO_2 inhalation task while blood-oxygenation-level-dependent (BOLD) magnetic resonance imaging (MRI) images were continuously collected. The cerebrovascular reactivity (CVR) index showed that the value of CVR in the WM (0.03 ± 0.002%/mm Hg) was positive, but was significantly lower than that in the gray matter (GM) (0.22 ± 0.01%/mm Hg). More strikingly, the WM response showed a temporal delay of 19 ± 3 seconds compared with GM, which was attributed to the longer time it takes for extravascular CO_2 to change. With age, WM CVR response becomes greater and faster, which is opposite to the changes seen in the GM. These data suggest that characteristics of WM CVR are different from that of GM and caution should be used when interpreting pathologic WM CVR results.

Journal of Cerebral Blood Flow & Metabolism (2014) **34,** 242–247; doi:10.1038/jcbfm.2013.194; published online 6 November 2013

Keywords: blood oxygenation level dependent; CO_2; hypercapnia; magnetic resonance imaging

INTRODUCTION

White matter (WM) comprises about half of the brain and is composed of bundles of myelinated nerve cell processes that connect various brain regions to each other.[1] White matter dysfunction is implicated in a number of neurologic diseases such as stroke,[2] Alzheimer's disease,[3] multiple sclerosis,[4] and traumatic brain injury.[5] At present, imaging studies of WM diseases primarily rely on *structural* imaging techniques, such as T_2-weighted MRI, diffusion tensor imaging, and magnetization transfer imaging.[6,7] Unfortunately, relatively little is known about the physiologic underpinnings that led to these alterations. Moreover, by the time structural changes can be detected, irreversible damage often has occurred and treatment options are limited. Physiologic changes usually take place before structure is altered, thus imaging of physiologic parameters may provide an early marker for disease diagnosis and progression. The present study aims to examine vascular parameters in the brain WM.

Compared with the gray matter (GM), vascular physiology of WM is still poorly understood. This is primarily because WM contains 70% to 75% less vasculature compared with GM,[8] resulting in a considerably lower signal-to-noise ratio.[9] Recent technical advances in imaging methodologies have mitigated some of these problems and provided the potential to examine vascular physiology in the WM.[10] For example, it has been suggested that baseline cerebral blood flow (CBF) of WM can be quantitatively assessed with arterial-spin-labeling (ASL) MRI on a region-by-region and tract-by-tract basis and that WM CBF is inversely correlated with diffusion fractional anisotropy.[10,11] The present study is focused on the examination of another important property of microvasculature: its ability to dilate on stimulation. This physiologic property, referred to as cerebrovascular reactivity (CVR),[12–14] is a critical function of healthy blood vasculature.[12,13] In the GM, this index has been measured using breath-hold,[15–19] pharmacological challenge with acetazolamide,[20] and inhalation of CO_2,[14,18,21] and is of great importance in functional MRI and its quantitative interpretation.[22–27] To date, CVR in the WM has not been studied systematically. Characterization of WM CVR may provide new insights into the mechanisms of ischemic and inflammatory responses in the WM, in particular in diseases such as multiple sclerosis[28] and stroke.[29] The knowledge of CVR may also improve our understanding of autoregulatory capacity of vasculature in the WM.

In the present study, we determined CVR by using CO_2 inhalation as a vasodilatory challenge and measured blood-oxygenation-level-dependent (BOLD) signal changes during this physiologic maneuver. Responses of WM CVR were examined in the context of both magnitude and temporal features. The most striking observation was that WM response to CO_2 inhalation was considerably delayed compared with that in the GM, and this was interpreted as the time it takes for the extravascular CO_2 to build up and reach a new steady state. The effect of age on these parameters was investigated by comparing WM CVR between younger and older participants. For comparison, baseline CBF in WM was also measured with ASL in these participants.

[1]Advanced Imaging Research Center, UT Southwestern Medical Center, Dallas, Texas, USA; [2]Biomedical Engineering Graduate Program, UT Southwestern Medical Center, Dallas, Texas, USA; [3]Department of Bioengineering, UT Arlington, Arlington, Texas, USA; [4]Department of Psychiatry, UT Southwestern Medical Center, Dallas, Texas, USA; [5]Center for Vital Longevity, UT Dallas, Dallas, Texas, USA and [6]Department of Radiology, Leiden University Medical Center, Leiden, The Netherlands. Correspondence: Dr H Lu, Advanced Imaging Research Center, UT Southwestern Medical Center, 5323 Harry Hines Boulevard, NE3.206, Dallas, TX 75390-8544, USA.
Email: hanzhang.lu@utsouthwestern.edu
This work was supported, in part, by the National Institutes of Health (R21 AG034318, R37 AG006265, R21 NS078656, R01 NS067015, R01 MH084021, and R01 AG042753).
Received 23 August 2013; revised 27 September 2013; accepted 8 October 2013; published online 6 November 2013

MATERIALS AND METHODS

Participants

This study was approved by the Institutional Review Board of the University of Texas Southwestern Medical Center and the University of Texas at Dallas, and was performed in accordance with the guidelines of the Declaration of Helsinki and Belmont Report. All subjects gave informed written consent before participation. Fifteen younger (age 27 ± 1.4 years, range 20 to 35 years, 5 males and 10 females) and fifteen older (age 75 ± 2 years, range 62 to 86 years, 8 males and 7 females) subjects were examined. Participants were recruited through flyers and advertisements in the local media. All participants recruited underwent extensive health screening and had no contraindications to MRI scanning (pacemaker, implanted metallic objects, and claustrophobia) and were generally in good health, with no serious or unstable medical conditions such as neurologic disease, brain injury, uncontrollable shaking, past bypass surgery or chemotherapy, or use of medications that affect cognitive function. All participants had a Mini-Mental-State-Exam[30] score of 26 or greater.

Experimental Procedures

Experiments were performed on a 3 Tesla MRI scanner using an 8-channel receive-only head coil (Philips Medical Systems, Best, The Netherlands). The body coil was used for radio frequency transmission. Foam padding was placed around the head to minimize motion during MRI scan acquisition.

Cerebrovascular reactivity was measured with a hypercapnia challenge, in which participants inhaled 5% CO_2 gas while BOLD MR images were simultaneously acquired. The details of the CVR measurement were described previously.[14] Briefly, during the CVR scan, subjects were fitted with a nose clip, and breathed room air and the prepared gas in an interleaved manner (60 seconds CO_2, 60 seconds room air, repeated three times) through a mouthpiece. The prepared gas was a mixture of 5% CO_2, 74% N_2, and 21% O_2 contained within a Douglas bag. The gas was delivered to the subject through a two-way non-rebreathing valve and mouthpiece combination (Hans Rudolph, 2600 series, Shawnee, KS, USA). A research assistant was inside the magnet room throughout the experiment to switch the valve and monitor the subject. Images of BOLD MR were acquired continuously during the entire experimental period. The end-tidal CO_2 (Et CO_2), the CO_2 concentration in the lung which approximates that in the arterial blood, was also recorded throughout the breathing task using a capnograph device (Capnogard, Model 1265, Novametrix Medical Systems, Wallingford, CT, USA). The total duration for the CVR scan was 7 minutes. The BOLD sequence used the following imaging parameters: single-shot echo planar imaging, field-of-view = 220 × 220 mm^2, matrix size = 64 × 64, 43 axial slices, thickness = 3.5 mm, no gap, repetition time/echo time/flip angle = 2,000 ms/25 ms/80°, and 210 volumes.

Baseline CBF was measured using a pseudo-continuous arterial-spin-labeling sequence, which has been shown to provide an improved sensitivity compared with previous ASL methods.[31,32] Scan parameters were pseudo-continuous labeling with a duration of 1.65 seconds, delay = 1.525 seconds, labeling radio frequency duration = 0.5 ms, pause between radio frequency pulses = 0.5 ms, labeling pulse flip angle = 18°, single-shot echo planar imaging, field-of-view = 240 × 240 mm^2, matrix = 80 × 80, 27 axial slices, thickness = 5 mm, repetition time/echo time = 4,020 ms/14 ms, 30 pairs of label and control images, duration 4 minutes.

In addition, a T_1-weighted high-resolution image was acquired using the Magnetization-Prepared-Rapid-Acquisition-of-Gradient-Echo (MPRAGE) sequence (voxel size = 1 × 1 × 1 mm^3, scan duration = 4 minutes).

Data Processing

Cerebrovascular reactivity data were analyzed using the software Statistical Parametric Mapping (SPM), (University College London, UK) and in-house MATLAB (MathWorks, Natick, MA, USA) scripts.[14] Pre-processing of the BOLD images included motion correction and registration with T_1-weighted anatomic images. The data were analyzed in individual space. This is because spatial normalization to standard space usually results in smoothing of the image, which could increase the partial voluming effect of GM on WM regions-of-interest (ROIs).

Quantitative analyses of the data have primarily focused on the ROI results as they are more reliable than voxelwise results in the WM. The WM ROI was defined using the following three steps to minimize GM contribution (Figure 1). In the first step, the T_1-weighted MPRAGE image was segmented (SPM5, University College London, UK) to obtain a WM probability map and only voxels with a WM probability of 90% or greater were included in the preliminary ROI. Second, recognizing that the BOLD resolution (3.4 × 3.4 × 3.5 mm^3) is considerably lower than MPRAGE and that there could be slight misregistration between BOLD and MPRAGE, we further eroded the preliminary WM ROI (i.e., peeling off a 1-mm layer) three-dimensionally by six times, resulting in a rather small but minimally contaminated WM ROI (see Figure 1 for an example). Finally, voxels inside WM lesions, which could occur in older adults, were excluded using T_2-weighted image that has been preregistered to the MPRAGE space. We found that only <1% of the voxels in our WM ROI (after erosion) was located in lesion regions, because lesion voxels were predominantly periventricular while our WM ROI consisted of primarily deep WM voxels. Blood-oxygenation-level-dependent time courses of the voxels within the final ROI were subsequently averaged. For comparison, a GM ROI was also delineated by selecting voxels with a GM probability of 90% or greater. These voxels were identified from a single slice immediately above the lateral ventricles, where it contains cortical GM only (no deep GM) and the coregistration between MPRAGE and BOLD images is highly reliable. Gray matter ROIs from other slices were also investigated, but no dependency of the results on sampling position was found.

From the averaged BOLD time course, two measures were obtained: the delay time and magnitude. Previous studies have established that the trace of end-tidal CO_2 and GM BOLD signal have a time shift of ~15 seconds,[14,33] which is the time it takes for the blood to travel from the lungs to the brain tissue and for the vessels in the tissue to react to the change in CO_2 concentration. This delay time may be different for WM, thus was specifically determined in the present study. The procedure was based on conducting a series of multiregression analyses with a range of delay times and identifying the delay that corresponds to the best fit. Specifically, in each regression analysis, the BOLD time course was used as the dependent variable, and the time-shifted Et CO_2 curve and a linear curve to account for BOLD signal drift were used as the independent variables (Figure 1). The range of Et CO_2 shift tested was from 0 to 60 seconds. A residual error was obtained for each regression analysis. The different regression analyses used an increasing amount of shift in Et CO_2. The shift that yielded the least residual errors was determined to be the optimal delay between Et CO_2 and the BOLD signal. Next, the magnitude of CVR was calculated using the coefficients from linear regression at the optimal delay,[14] and is written in %BOLD signal per mm Hg. The above analyses were conducted separately for GM and WM time courses.

Arterial-spin-labeling MR images were used to calculate a quantitative CBF map by subtraction of the control and label image sets following procedures established previously.[34] The 30 repeated scans were averaged to improve the signal-to-noise ratio. The WM and GM ROIs described were applied to the ASL data to obtain baseline CBF values in these regions.

Statistical Analysis

All parametric values are reported in mean ± standard error. Data from younger and older groups were compared with a two-sample Student's *t*-test. The GM and WM results were compared with a paired Student's *t*-test. A *P* value of 0.05 or less is considered as significant.

Exploratory Analysis on the Curvature Differences Between White Matter and Gray Matter Time Courses

In the regression analysis, the temporal differences in WM and GM time courses have mainly been modeled as simple time shift. Another possibility is that the two signals could have different curvatures. Specifically, the WM time course may have a smoother and broader response compared with the GM due to dispersion of the bolus in WM vasculature.[35] We therefore tested this possibility by convolving the GM time courses, $Y_{GM}(t)$, with a mono-exponential 'dispersion' function, $d(t) = e^{-t/\tau}$, to yield a smoothed version of the GM time course, $\bar{Y}_{GM}(t) = Y_{GM}(t) \otimes d(t)$. Multiregression analysis was then performed in which $Y_{WM}(t)$ was used as the dependent variable and $\bar{Y}_{GM}(t)$ was the independent variable and a linear term was a covariate, similar to that shown in Figure 1. This regression analysis was performed for a range of τ values (0 to 60 seconds) in the dispersion function. The optimal value for the time constant τ was determined based on minimal residual errors.

RESULTS

Volumes of WM ROI were 10.9 ± 1.0 cm^3 ($N = 15$) and 5.7 ± 1.0 cm^3 ($N = 15$) in younger and older participants, respectively. Both were sufficiently large for accurate signal estimation, although the

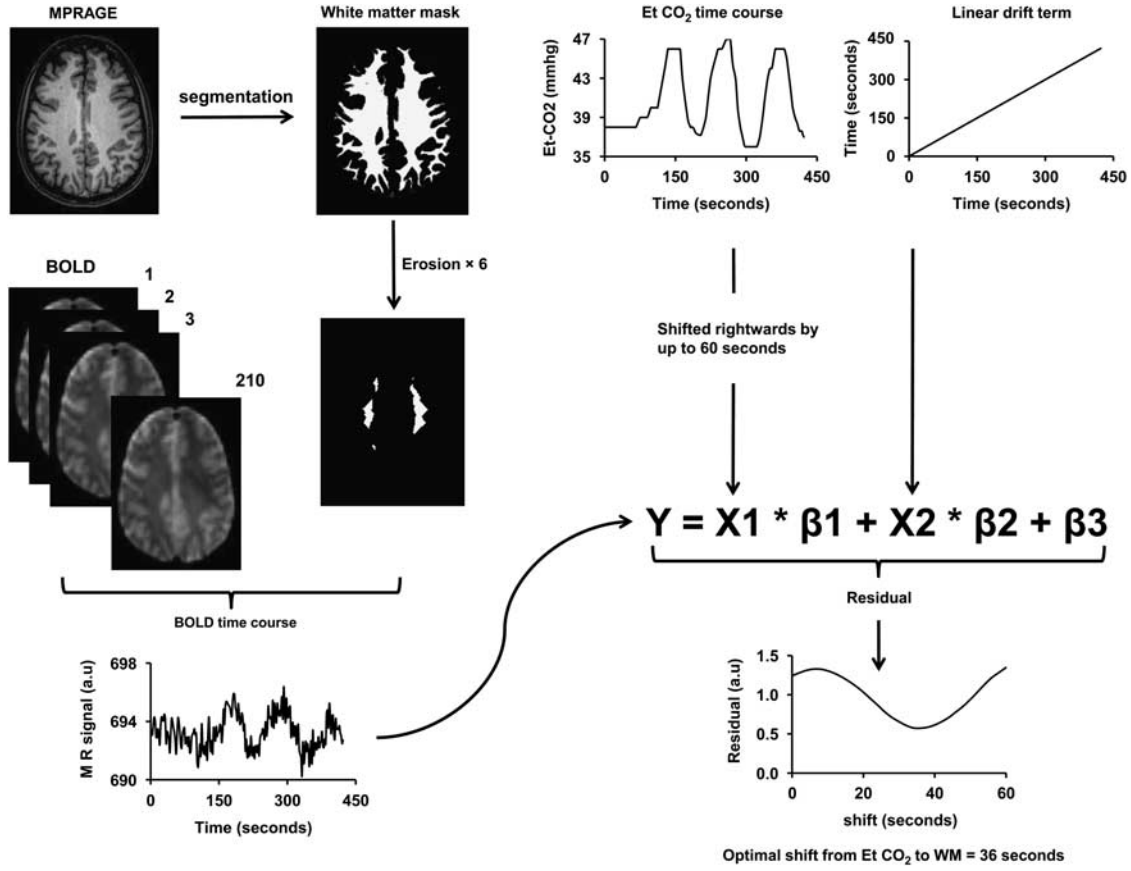

Figure 1. Illustration of analysis steps for the quantification of white matter (WM) cerebrovascular reactivity (CVR) and delay time. Upper left: Magnetization-Prepared-Rapid-Acquisition-of-Gradient-Echo (MPRAGE) T_1-weighted image is segmented using SPM5 to obtain a mask of WM (voxels with >90% WM probability). To further reduce the likelihood of gray matter (GM) partial volume, the mask is eroded three-dimensionally by six times. Thus, the final mask is considerably small, but is expected to contain minimal GM contribution. The final mask is then applied on the blood-oxygenation-level-dependent (BOLD) image series to obtain a BOLD time course in the WM, which is used as the dependent variable in the linear regression analysis. Upper right: End-tidal (Et) CO_2 time course and a linear drift term are used as independent variables in the linear regression analysis. To identify the optimal delay time, the Et CO_2 curve is shifted rightwards by 0 to 60 seconds at an interval of the acquisition repetition time (TR) (2.0 seconds). At each shift, the linear regression analysis was performed and a residual error term is calculated. The optimal delay time is then determined based on the shift that yields the least residual error.

younger group had a significantly greater volume ($P<0.001$). The average WM probability of these ROIs was 0.9989 ± 0.0001 and 0.9981 ± 0.0003 for younger and older subjects, respectively, suggesting that GM partial volume was minimal. Volumes of GM ROI were 5.0 ± 0.1 and $3.86 \pm 0.08\,cm^3$ in younger and older subjects, respectively.

Average time courses of Et CO_2, GM, and WM BOLD signals in young subjects are shown in Figure 2a. The most interesting feature is that there is a clear temporal delay in the WM time course relative to the GM. Table 1 summarizes the quantitative results. It can be seen that, in young subjects, GM signal lags behind the Et CO_2 time course by $\sim$15 seconds, which is in agreement with the previous literature.[14,33] In the WM, BOLD signal appears to manifest a further and drastic delay of 19 seconds, compared with the GM. The magnitude of WM CVR was $14 \pm 1\%$ of that in the GM ($P<0.001$).

End-tidal CO_2, GM, and WM BOLD signals in older subjects are shown in Figure 2b. Cerebrovascular reactivity parameters in older subjects showed several important differences from that in young. First, the lag between Et CO_2 and GM time courses in elderly was significantly greater ($P=0.003$) than that in young (Table 1). Second, the delay between GM and WM BOLD time course is considerably shorter in elderly (from 19 seconds in young to 8 seconds in elderly, $P=0.002$). Moreover, the magnitude of WM

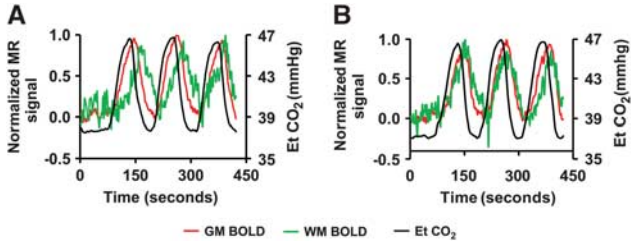

Figure 2. Time courses of End-tidal (Et) CO_2, gray matter (GM) blood-oxygenation-level-dependent (BOLD), and white matter (WM) BOLD signal in (**A**) younger and (**B**) older subjects. To highlight the timing differences, the magnetic resonance (MR) signals have been normalized such that normocapnic signal is 0 and hypercapnic signal is 1. The Et CO_2 values are plotted in units of mm Hg (right axis). It can be seen that the WM time courses lag behind the GM signal, which in turn lags behind the Et CO_2. The curves were obtained from averaging across all subjects. Error bars are not plotted for clarity of the figure.

CVR was found to be greater ($P=0.003$) in older than in younger subjects (Table 1). As a result, the WM/GM CVR ratio in elderly was $29 \pm 2.7\%$, much greater ($P<0.001$) than that in young ($14 \pm 1\%$ as

Table 1. Summary of CVR and CBF results in the GM and WM ROIs ($N = 15$ for younger group; $N = 15$ for older group)

	CVR delay (seconds)			*CVR magnitude (% BOLD/mm Hg CO_2)*		*CBF (mL/100 g per minute)*		
Group	*Et CO_2 to GM*	*Et CO_2 to WM*	*GM to WM*	*GM*	*WM*	*GM*	*WM*	*WM/GM ratio*
Young ($N = 15$)	15.3 ± 0.6	34.4 ± 2.9	19.1 ± 3.0	0.22 ± 0.01	0.03 ± 0.002	68.2 ± 2.5	15.9 ± 0.8	0.23 ± 0.01
Old ($N = 15$)	18.5 ± 0.8	26.9 ± 1.3	8.4 ± 1.0	0.17 ± 0.01	0.05 ± 0.005	52.9 ± 2.8	18.8 ± 1.8	0.35 ± 0.02
P value	0.003	0.029	0.002	< 0.001	0.003	< 0.001	0.152	< 0.001

BOLD, blood-oxygenation-level-dependent; Et CO_2, end-tidal CO_2; CBF, cerebral blood flow; CVR, cerebrovascular reactivity; GM, gray matter; ROIs, regions-of-interest; WM, white matter.
Data are presented in mean ± standard error. *P* values listed are based on each comparison and are not corrected for multiple comparisons.

described above). Baseline CBF data showed similar trends (Table 1) in that the WM/GM CBF ratio in elderly (35 ± 2%) was greater ($P < 0.001$) than that in young (23 ± 0.9%). Finally, GM CVR in elderly was significantly lower ($P < 0.001$) than that in young, which is relatively well established from the previous literature.[36,37]

Further analysis was performed to test the possibility that the WM time course is best matched by the convolution of the GM time course with an exponential dispersion function, rather than by simply shifting the GM time course. The optimal time constant for the exponential function was found to be 26 ± 5 and 8 ± 2 seconds for younger and older subjects, respectively, with a significant group difference ($P = 0.004$). The convolution analysis yielded slightly lower ($P = 0.038$) residual error (1.4 ± 0.3 in units of MR signal) than the shift analysis (1.7 ± 0.3).

DISCUSSION

The present study conducted a systematic examination of CVR in the WM and its dependence on age. Our data suggested that, in addition to the expected difference in response magnitude, CVR in the WM is different from that in the GM in several important aspects. Furthermore, while the amplitude of reactivity decreases with age in the GM, the opposite pattern is seen in the WM.

One of the main findings of the present study is that CVR response in the WM is considerably slower than that in the GM, consistent with a slower rise time reported by Rostrup *et al.*[13] Using the shift analysis, we found that the WM response lags behind the GM by 19 seconds in young individuals. Using a different analysis based on the dispersion, it was found that the WM signal is equivalent to the GM signal smoothed by an exponential function with a time constant of 26 seconds. This is surprising considering that the WM ROI is located just a few centimeters deeper than the GM. Of course, it is well known that blood arrives later in the WM than in the GM due to the known anatomy of the vasculature.[35] However, evidence from ASL and DSC-MRI literature suggests that this should only be 2 to 3 seconds at most.[38] Therefore, we hypothesize that this large delay is primarily due to a slow response of the WM compared with the GM. Specifically, we propose that it takes considerable amount of time for the extravascular CO_2 in the WM to build up and reach a new steady state, after the arterial CO_2 content has been altered. Figure 3 shows a qualitative illustration of this potential mechanism. The longer buildup time is primarily attributed to a low CBF in the WM, such that the amount of additional CO_2 that is brought to the WM per unit time is relatively small. Given the large fraction of tissue in the WM (98% tissue, 2% blood), it is plausible that it takes tens of seconds for the extravascular CO_2 concentration to change. It should also be noted that hypercapnia-induced vasodilation is primarily mediated by extravascular CO_2 concentration rather than intravascular CO_2. This notion is derived from animal data that selective inhibition of vascular endothelium function does not reduce hypercapnic response whereas inhibition of neuronal nitric oxide synthase does.[39]

Another interesting finding of the present study is that WM in the older subjects showed a faster CVR response compared with young, such that the GM-to-WM delay in elderly is not as pronounced as those in young. Following our proposed mechanism described in the previous paragraph, this would mean that extravascular CO_2 concentration in the WM of older individuals increases more rapidly upon a change in arterial CO_2 content. This prediction is consistent with the baseline CBF results that WM CBF was greater in older than in younger subjects, thus it takes less time for the CO_2 to build up. The reason that WM CBF and CVR are greater in elderly than in young may be associated with the mechanical properties of the WM. White matter in young subjects is tightly packed with axons and myelin, which makes it difficult for blood to penetrate and for vessels to dilate. This notion is supported by recent findings that, within healthy brain, fiber tracts that have higher fractional anisotropy (i.e., tighter organization with more myelin) tend to have a lower CBF.[11] In older individuals, as age-related demyelination and axon loss takes place, WM becomes less densely packed, thus exhibiting less hindrance for blood to flow through loose WM fibers.

Characteristics of WM CVR have been discussed in two previous studies. Mandell *et al*[40] reported that WM CVR could actually be negative (i.e., BOLD signal decreases with CO_2 inhalation), especially in WM regions adjacent to lateral ventricles. The authors interpreted these findings as a steal phenomenon by the GM in response to hypercapnia. Blockley *et al*[33] showed in a voxel-by-voxel analysis that WM CVR had a considerable delay, similar to those shown in this study. However, the authors were not able to rule out the possibility of estimation errors and considered these as artifacts due to low signal-to-noise ratio in their data.[33] In the present study, we have used several procedures to improve the reliability of our data. First, we have focused our analysis on ROI results, which have greater signal-to-noise ratio compared with single-voxel results. Second, to ensure that the voxels included in the ROI are indeed WM voxels and to minimize partial volume of GM, we used tissue segmentation in combination with ROI erosion such that only the core of the WM region is included in the final ROI. Third, we have used a shift-based analysis, in which the range of shifts tested included both shorter and longer than the expected GM delay. Thus, if noise had caused a difference in GM and WM timing, then we should at least observe the WM time course leading the GM in some (e.g., 25%) subjects, which we did not see. Finally, we studied two separate groups of subjects (younger and older) and both showed a significant GM-versus-WM difference. Thus, the probability of random noise to cause the same false positive observation in two studies is relatively low.

The results in this study have several practical implications for the design and analysis of CVR studies. First, given the considerable differences in delay times between tissue types, frequency-domain data analysis[33] may be a preferred approach

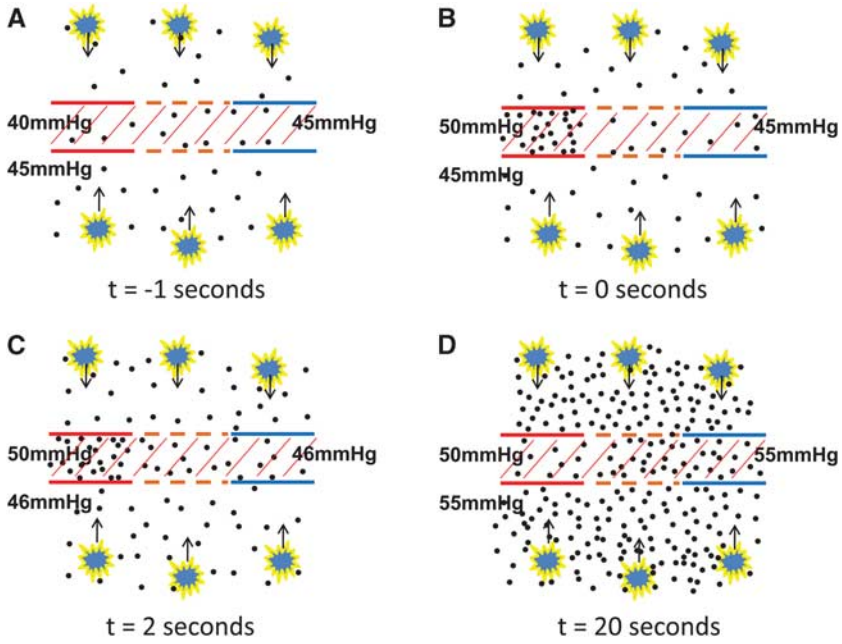

Figure 3. A proposed mechanism to explain the delay in cerebrovascular reactivity (CVR) response in the white matter (WM). (**A**) Under normocapnic steady state, arterial CO_2 partial pressure is ~40 mm Hg and tissue CO_2 is ~45 mm Hg. Red lines indicate arterial vessel wall. Brown color denotes capillary vessel wall, which is shown as dashed lines to indicate that it is permeable to CO_2 molecules. Blue lines indicates venous vessel wall. It is assumed that tissue and blood CO_2 concentrations have reached equilibrium in capillary, thus venous CO_2 pressure is the same as tissue CO_2. Hatched area indicates intravascular space. Black dots illustrate CO_2 molecules. The yellow symbols indicate tissue cells, which generate CO_2 and the arrows indicate that CO_2 generated by tissue is cleared through blood vessels. (**B**) When the hypercapnic blood first arrives, arterial CO_2 concentration will increase, delivering extra CO_2 to the tissue. (**C**) However, tissue and venous CO_2 pressure shows a much slower change than the arterial CO_2, due to the large space of tissue compared with the rate of blood flow. Note that, with a perfusion of 30 mL/100 g per minute, the amount of blood delivered to the WM per second is only 0.5% of the tissue space. Therefore, during the first few seconds after the arterial CO_2 has changed, extravascular CO_2 may not show a pronounced alteration. (**D**) With time, extravascular CO_2 concentration increases substantially and a new steady state is reached.

over time-domain analysis, as it is less sensitive to the delay in time course. Second, it is desirable to use a breathing paradigm that could generate a BOLD time course of an approximate sinusoidal function, so that the time course would have a prominent frequency peak. To achieve this, one can use a feedback/feedforward system targeting for a sinusoidal curve.[33] Alternatively, one can use a fixed inspired O_2 method with a short period (e.g., switching gas every minute).[14] Due to the mixing of gas bolus in the lung and dispersion of blood bolus along its path to the brain, the BOLD time course with this paradigm is also generally similar to a sinusoidal curve. Third, high temporal resolution in data acquisition (e.g., short repetition time) is desired to accurately depict time delays in the signal. Finally, when evaluating WM CVR data under pathologic conditions, potential change in both amplitude and temporal features should be considered. Note that, if the delay time is not properly accounted for, the response amplitude may be underestimated leading to mis-interpretation of results.

For the quantification of timing difference between the WM and GM BOLD time courses, we used two analysis methods, one based on shifting the time course and the other based on convolution of the time course with an exponential dispersion function. From our mechanistic model proposed in Figure 3, the dispersion and smoothing of the WM response relative to GM seem more plausible. Additionally, the convolution analysis yielded lower residual error compared with the shift analysis, again supporting the dispersion method. However, given that the WM BOLD time course is generally variable and the residual error is of similar amplitude using the two analyses, the exact determination of the optimal analysis method as well as the physiologic interpretation requires further investigation. A limitation of the present study is that the gender distributions in the younger and older groups were not exactly matched. The older group had more male subjects. It is known that females and males could have different blood flow. Therefore, some of the CBF findings (e.g., lower GM CBF in old) could be influenced by this confounding factor.

Conclusions

White matter CVR in response to hypercapnia is different from that of GM in several important aspects. Aside from the expected reduction in magnitude, WM response was slower than GM by tens of seconds. This may be attributed to the longer time it takes for WM extravascular CO_2 to accumulate and may be related to the lower perfusion in this tissue type. With age, WM CVR becomes greater and faster, which is opposite to the changes seen in the GM.

DISCLOSURE/CONFLICT OF INTEREST

The authors declare no conflict of interest.

REFERENCES

1 Waxman SG, Kocsis JD, Stys PK. *The Axon: Structure, Function and Pathophysiology*. 1st ed. Oxford University Press: New York, NY, 1995.
2 Hui ES, Fieremans E, Jensen JH, Tabesh A, Feng W, Bonilha L *et al.* Stroke assessment with diffusional kurtosis imaging. *Stroke* 2012; **43**: 2968–2973.
3 Kantarci K, Jack Jr CR, Xu YC, Campeau NG, O'Brien PC, Smith GE *et al.* Mild cognitive impairment and Alzheimer disease: regional diffusivity of water. *Radiology* 2001; **219**: 101–107.

4 Inglese M, Bester M. Diffusion imaging in multiple sclerosis: research and clinical implications. *NMR Biomed* 2010; **23**: 865–872.
5 Lipton ML, Gulko E, Zimmerman ME, Friedman BW, Kim M, Gellella E *et al.* Diffusion-tensor imaging implicates prefrontal axonal injury in executive function impairment following very mild traumatic brain injury. *Radiology* 2009; **252**: 816–824.
6 Wakana S, Jiang H, Nagae-Poetscher LM, van Zijl PC, Mori S. Fiber tract-based atlas of human white matter anatomy. *Radiology* 2004; **230**: 77–87.
7 Pike GB, De Stefano N, Narayanan S, Worsley KJ, Pelletier D, Francis GS *et al.* Multiple sclerosis: magnetization transfer MR imaging of white matter before lesion appearance on T2-weighted images. *Radiology* 2000; **215**: 824–830.
8 Lu H, Law M, Johnson G, Ge Y, van Zijl PC, Helpern JA. Novel approach to the measurement of absolute cerebral blood volume using vascular-space-occupancy magnetic resonance imaging. *Magn Reson Med* 2005; **54**: 1403–1411.
9 van Gelderen P, de Zwart JA, Duyn JH. Pittfalls of MRI measurement of white matter perfusion based on arterial spin labeling. *Magn Reson Med* 2008; **59**: 788–795.
10 van Osch MJ, Teeuwisse WM, van Walderveen MA, Hendrikse J, Kies DA, van Buchem MA. Can arterial spin labeling detect white matter perfusion signal? *Magn Reson Med* 2009; **62**: 165–173.
11 Aslan S, Huang H, Uh J, Mishra V, Xiao G, van Osch MJ *et al.* White matter cerebral blood flow is inversely correlated with structural and functional connectivity in the human brain. *Neuroimage* 2011; **56**: 1145–1153.
12 Kastrup A, Kruger G, Neumann-Haefelin T, Moseley ME. Assessment of cerebrovascular reactivity with functional magnetic resonance imaging: comparison of CO(2) and breath holding. *Magn Reson Imaging* 2001; **19**: 13–20.
13 Rostrup E, Law I, Blinkenberg M, Larsson HB, Born AP, Holm S *et al.* Regional differences in the CBF and BOLD responses to hypercapnia: a combined PET and fMRI study. *Neuroimage* 2000; **11**: 87–97.
14 Yezhuvath US, Lewis-Amezcua K, Varghese R, Xiao G, Lu H. On the assessment of cerebrovascular reactivity using hypercapnia BOLD MRI. *NMR Biomed* 2009; **22**: 779–786.
15 Murphy K, Harris AD, Wise RG. Robustly measuring vascular reactivity differences with breath-hold: normalising stimulus-evoked and resting state BOLD fMRI data. *Neuroimage* 2011; **54**: 369–379.
16 Kannurpatti SS, Motes MA, Rypma B, Biswal BB. Non-neural BOLD variability in block and event-related paradigms. *Magn Reson Imaging* 2011; **29**: 140–146.
17 Zaca D, Hua J, Pillai JJ. Cerebrovascular reactivity mapping for brain tumor presurgical planning. *World J Clin Oncol* 2011; **2**: 289–298.
18 Tancredi FB, Hoge RD. Comparison of cerebral vascular reactivity measures obtained using breath-holding and CO2 inhalation. *J Cereb Blood Flow Metab* 2013; **33**: 1066–1074.
19 Bright MG, Murphy K. Reliable quantification of BOLD fMRI cerebrovascular reactivity despite poor breath-hold performance. *Neuroimage* 2013; **83C**: 559–568.
20 Bokkers RP, van Osch MJ, van der Worp HB. de Borst GJ, Mali WP, Hendrikse J. Symptomatic carotid artery stenosis: impairment of cerebral autoregulation measured at the brain tissue level with arterial spin-labeling MR imaging. *Radiology* 2010; **256**: 201–208.
21 Wise RG, Pattinson KT, Bulte DP, Chiarelli PA, Mayhew SD, Balanos GM *et al.* Dynamic forcing of end-tidal carbon dioxide and oxygen applied to functional magnetic resonance imaging. *J Cereb Blood Flow Metab* 2007; **27**: 1521–1532.
22 Hoge RD, Atkinson J, Gill B, Crelier GR, Marrett S, Pike GB. Linear coupling between cerebral blood flow and oxygen consumption in activated human cortex. *Proc Natl Acad Sci USA* 1999; **96**: 9403–9408.
23 Sicard KM, Duong TQ. Effects of hypoxia, hyperoxia, and hypercapnia on baseline and stimulus-evoked BOLD, CBF, and CMRO2 in spontaneously breathing animals. *Neuroimage* 2005; **25**: 850–858.
24 Uludag K, Dubowitz DJ, Yoder EJ, Restom K, Liu TT, Buxton RB. Coupling of cerebral blood flow and oxygen consumption during physiological activation and deactivation measured with fMRI. *Neuroimage* 2004; **23**: 148–155.
25 Zappe AC, Uludag K, Logothetis NK. Direct measurement of oxygen extraction with fMRI using 6% CO2 inhalation. *Magn Reson Imaging* 2008; **26**: 961–967.
26 Chen JJ, Pike GB. MRI measurement of the BOLD-specific flow-volume relationship during hypercapnia and hypocapnia in humans. *Neuroimage* 2010; **53**: 383–391.
27 Chen JJ, Pike GB. Global cerebral oxidative metabolism during hypercapnia and hypocapnia in humans: implications for BOLD fMRI. *J Cereb Blood Flow Metab* 2010; **30**: 1094–1099.
28 Iannetti GD, Wise RG. BOLD functional MRI in disease and pharmacological studies: room for improvement? *Magn Reson Imaging* 2007; **25**: 978–988.
29 Mandell DM, Han JS, Poublanc J, Crawley AP, Stainsby JA, Fisher JA *et al.* Mapping cerebrovascular reactivity using blood oxygen level-dependent MRI in patients with arterial steno-occlusive disease: comparison with arterial spin labeling MRI. *Stroke* 2008; **39**: 2021–2028.
30 Folstein MF, Folstein SE, McHugh PR. "Mini-mental state". A practical method for grading the cognitive state of patients for the clinician. *J Psychiatr Res* 1975; **12**: 189–198.
31 Wong EC. Vessel-encoded arterial spin-labeling using pseudocontinuous tagging. *Magn Reson Med* 2007; **58**: 1086–1091.
32 Dai W, Garcia D, de Bazelaire C, Alsop DC. Continuous flow-driven inversion for arterial spin labeling using pulsed radio frequency and gradient fields. Magn Reson Med 2008; **60**: 1488–1497.
33 Blockley NP, Driver ID, Francis ST, Fisher JA, Gowland PA. An improved method for acquiring cerebrovascular reactivity maps. *Magn Reson Med* 2011; **65**: 1278–1286.
34 Alsop DC, Detre JA. Reduced transit-time sensitivity in noninvasive magnetic resonance imaging of human cerebral blood flow. *J Cereb Blood Flow Metab* 1996; **16**: 1236–1249.
35 Duvernoy HM, Delon S, Vannson JL. Cortical blood vessels of the human brain. *Brain Res Bull* 1981; **7**: 519–579.
36 Lu H, Xu F, Rodrigue KM, Kennedy KM, Cheng Y, Flicker B *et al.* Alterations in cerebral metabolic rate and blood supply across the adult lifespan. *Cereb Cortex* 2011; **21**: 1426–1434.
37 D'Esposito M, Deouell LY, Gazzaley A. Alterations in the BOLD fMRI signal with ageing and disease: a challenge for neuroimaging. *Nat Rev Neurosci* 2003; **4**: 863–872.
38 Liu P, Uh J, Devous MD, Adinoff B, Lu H. Comparison of relative cerebral blood flow maps using pseudo-continuous arterial spin labeling and single photon emission computed tomography. *NMR Biomed* 2011; **25**: 779–786.
39 Brian Jr JE. Carbon dioxide and the cerebral circulation. *Anesthesiology* 1998; **88**: 1365–1386.
40 Mandell DM, Han JS, Poublanc J, Crawley AP, Kassner A, Fisher JA *et al.* Selective reduction of blood flow to white matter during hypercapnia corresponds with leukoaraiosis. *Stroke* 2008; **39**: 1993–1998.